

Article

Electric Field-Based Ozone Nanobubbles in Tandem with Reduced Ultraviolet Light Exposure for Water Purification and Treatment: Aquaculture and Beyond

Niall J. English 

School of Chemical and Bioprocess Engineering, University College Dublin, Belfield, D04 V1W8 Dublin, Ireland; niall.english@ucd.ie

Abstract: Micro- and nanobubbles are tiny gas bubbles that are smaller than 100 μm and 1 μm , respectively. This study investigated the impact of electric field ozone nanobubbles (EF-ONBs) on the purification of both deionised and aquaculture water bodies, finding that heightened reactive oxygen species (ROS) production and oxygen reduction potential (ORP) are correlated to a higher production of EF-ONBs. In particular, it was found that there were substantially reduced ultraviolet light requirements for aquaculture when using EF-ONBs to maintain aquaculture purification standards. It is clear that the approximately exponential decay is slowed down by almost ten times by EF-ONBs even without UV applied, and that it is still roughly six times longer than the ‘control’ case of standard O_3 sparging in water (i.e., meso- and macro-bubbles with no meaningful level of dispersed-phase, bubble-mediated dissolution beyond the standard Henry’s law state—owing mostly to rapid Stokes’ law rising speeds). This has very positive implications for, *inter alia*, recirculation aeration systems featuring an ozonation cycle, as well as indoor agriculture under controlled-light environments and malting, where ozonation cycles are also often used or contemplated in process redesign strategies. Such promising results for EF-ONBs offer, *inter alia*, more sustainable aquaculture, water sterilisation, indoor farming, and malting.



Citation: English, N.J. Electric Field-Based Ozone Nanobubbles in Tandem with Reduced Ultraviolet Light Exposure for Water Purification and Treatment: Aquaculture and Beyond. *Environments* **2024**, *11*, 292. <https://doi.org/10.3390/environments11120292>

Academic Editor: Chien-Sen Liao

Received: 23 November 2024

Revised: 16 December 2024

Accepted: 17 December 2024

Published: 18 December 2024



Copyright: © 2024 by the author. Licensee MDPI, Basel, Switzerland. This article is an open access article distributed under the terms and conditions of the Creative Commons Attribution (CC BY) license (<https://creativecommons.org/licenses/by/4.0/>).

Keywords: O_3 nanobubbles; aquaculture; sustainable agriculture; ultraviolet

1. Introduction

The pressing need to make wastewater treatment much more sustainable is urgent due to the growing global population, ongoing difficulties brought on by climate change, and depletion of natural resources, particularly vis-à-vis energy consumption [1]. Water sources once considered safe and sustainable may be becoming increasingly less so—such as, *inter alia*, exploitation of aquifer water no longer being reliable [2]—so more sustainable water sourcing and treatment approaches are essential, e.g., the US EPA’s Final Long-Term 1 Enhanced Surface-Water Treatment rule (LT1ESWTR) [3]. Applying O_3 and ultraviolet (UV) radiation together is especially effective—to treat pathogenic organisms in water wastewater systems [4–6], with inactivation using both UV and O_3 [7,8]. The application of O_3 is a critical step for safely realising bottled water purification standards and best-in-class clean-in-place sanitation, as well as the processing of produce, meat, and industrial reuse—and, increasingly in recent years, in aquaculture, especially as a step in some recirculation aeration systems [9]. Barley malting is another emerging application wherein O_3 step application is becoming more important and developing in technical maturity [10]. However, there are, of course, operational and economic challenges in large-scale ozonation, with or without the parallel application of UV—not least boosting dissolved O_3 levels, and, especially, solvated O_3 lifetime [11]—especially on the pressurised injection of O_3 into a UV-exposed stirred-tank reactor, with the resultant production of micro- and meso-bubbles—renewing continuously the gas-to-liquid mixing zone and boosting gas solubility to maximise the usage of the incident UV irradiation [12].

Certain pollutants, such as cyanide and pesticides, oxidise more quickly at higher pH levels because O_3 can be converted to hydroxyl more easily. To achieve maximal efficiency in system design and control requires careful consideration of the balance between the pH level, UV photolysis, and O_3 dosage: *ceteris paribus*, there is an average radiation power at which the oxidation efficiency is maximised for a given ozonation addition rate [13]. Indeed, combined O_3 /UV treatment has led to a substantial reduction in dye levels in the textile industry, whilst in certain dyes, O_3 and UV radiation also demonstrated a greater capacity to influence mineralisation and toxic reduction [14,15]. Using O_3 and UV light to degrade and decompose surfactants, as well as emulsifying and chelating agents, has proven to be more successful than biological treatments for these widely used industrial substances, like anionic surfactants: the hydroxyl radical starts chain reactions that eventually result in mineralisation at low pH levels, whilst the electrophilic attack of O_3 breaks down organic compounds [16]. In addition, O_3 and/or UV treatment can rapidly remove the nitrogen or chlorine atoms from the benzene ring, facilitating a more thorough phenol breakdown. For instance, combined O_3 /UV can remove 99 percent of 2,4-dichlorophenol, 2-chlorophenol, and 2-nitrophenol in roughly 15 min [17]; it is the combination of both treatments that is so effective [17]. Indeed, kinetic studies have indicated that the rate at which organics oxidise by ozonation increases by 10- to 10,000-fold in tandem with the increase in UV exposure intensity, with O_3 -mediated degradation reaction rates *per se* increasing 10- to 1000-fold as the UV strength increases, in the case of O_3 -resistant compounds, such as, *inter alia*, acids, alcohols, amino acids, and fatty acids [18].

Clearly, and as noted in the discussion above, any method that prolongs such “active life” of O_3 , as well as boosting dissolved O_3 levels (and, as a “spin-off” benefit, dissolved O_2 levels too—*vide infra*) would be enormously welcome [19]. The novelty and originality of the present study is that it achieves exactly that by leveraging large populations of dense and electric field-generated nanobubbles (NBs) to prolong this activity.

In terms of the urgency in addressing food and water sustainability and security concerns and optimising crop productivity, nanobubbles (NBs) have emerged as one prominent subject of research within water treatment innovations and long-term aeration [20–22]. Bearing in mind the encouraging progress of O_3 nanobubbles in water disinfection, despite the abovementioned fundamental concerns hampering more widespread industrial/agricultural/aquacultural adoption (*i.e.*, limited solubility and faster-than-desired auto-degradation kinetics) [23–25], the purpose of the present study generates dense, electric field-generated nanobubbles [20], which, unlike traditional mechanical generation approaches for NBs, are proven to both boost dissolved gas levels and longevity by way of their inherent metastability and greatly slowed Stokes’ law rising in an energy-efficient way [22]. This is radically different—and more ambitious—than the status quo (*ante*) of short-lived ozone and parallel energy-intensive supply of UV to ozonate water—and far more energy-efficient. Crucially, for the first time, the present study achieves this with and without the application of UV irradiation, to both deionised and aquaculture water sources. Outside of realising cleaner, disinfected water, *per se*, a particular sector of interest for O_3 electric field nanobubbles (EF-ONBs) is aquaculture, wherein longer-lasting, potent O_3 NBs may penetrate cell wall matrices in shellfish to eliminate viruses (which are a serious risk in contaminated waters), *e.g.*, norovirus, as well as cell-wall penetration in (more light-efficient) indoor agriculture and barley malting to dispose of similar intra-cellular viruses. An additional goal of the present study, owing to the energy-efficient nature of EF-NB generation [20–22], is to use solar energy for this purpose for even greater sustainability—taking inspiration, in part, from recent trends in the literature and industry for off-grid ozonation efforts [26].

The present study is organised as follows: in Section 2, we describe the mechanism of NB generation by the novel electric-field approach as well as the experimental set-ups for ozonation by means of NBs, whilst Section 3 reviews water characterisation approaches in the presence of ozone NBs and reviews UV exposure operations. Sections 4 and 5 discuss norovirus assessment methods and the concomitant approach to determine reactive oxygen species (ROS). Finally, Section 6 discusses in detail the findings of ozone NB operations in

the context of UV-exposure reduction, whilst also considering wider aquaculture benefits, with 7 and 8 referring to norovirus and ROS-photoluminescence findings. Section 9 offers some important conclusions of this novel work—not only on aquaculture, per se, but also in the wider realm of novel and energy-efficient oxidative processes for water-treatment operations more generally.

2. Materials and Methods

Nanobubble Generation

O_3 nanobubbles were generated in very large quantities (and density per unit volume) via a submerged NB generator through an electric field approach [20], provided by AquaB Nanobubble Innovations Ltd. (Ireland, www.aquab.com, accessed on 1 November 2024). The NB-generation process was triggered by applying a DC voltage of 48 V (with sub-milliAmp current levels, ~ 0.05 mA), as per Figure 1, while O_3 was injected into the 5-litre water system (open to atmosphere, albeit under a fume hood); the submersible NB generator featured an internal diffuser. In more detail as to the NB generation method, per se, this is accomplished by the electrostriction approach (cf. Figure 1), whereby the static electric field induces a densification in the water surrounding larger macro- and meso-bubbles: in this way, this induces a temporary vacuum and negative-pressure region surrounding the “mother” population of bubbles—“sucking in” pockets, or packets, of gas into a “daughter sub-population” of satellite, nano-scale bubbles in the hydration-layer milieux enveloping the macro- and meso-bubbles. The DC power was obtained through a solar panel linking to a 70 Ah battery, with a transformer/inverter to provide 48 V DC and power a small gas pump (~ 5 W). Although the power draw of EF-meditated NB generation per se is close to zero, with solar/battery/transformer/inverter power losses of the order of 5 W, the total power inventory was therefore about 10 W. O_3 generation (powered separately by mains electricity) was ~ 5 g/h, enforced using a mass flow controller, and the gas (air and O_3) flow rate was about 5 litres per minute (STP). The meso-bubbles generated by the internal-to-generator diffuser rose by Stokes’ law through the DC electric-field milieu inside the NB generator, creating a sub-population of EF-ONBs, which diffused throughout the body of water. Initially, deionised (DI) water was used, and then a sample of shellfish farm water (sans shellfish), and the experiments were carried out in the presence and absence of a portable 365 nm, 50 W UV-A lamp (~ 1.5 mW/cm 2), mounted 5 cm above the water vessel. Each EF-ONB generation experiment was carried out for 15 min, for the 2×2 situations (DI/shellfish farm water, with/without UV exposure).

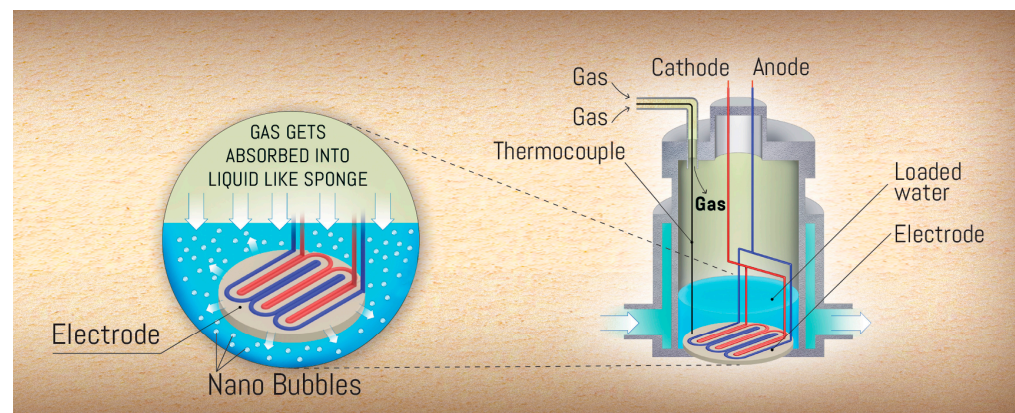


Figure 1. Schematic showing electric-field generation of nano-bubbles. (Image Credit: Jon Tallon).

A larger-scale, pilot-type study was carried out in a tank of ~ 3500 litres of shellfish farm water (again, without shellfish present) with ~ 50 g/h ozone generation and a gas flow of 25 litres per minute (STP), using a higher-intensity ~ 10 mW/cm 2 UV-A lamp (~ 3 kW, 365 nm). The tank was 1.45×1.8 m in cross-section, and the depth of the water therein was about 1.35 m. NB generation was carried out for 1 h, with and without UV exposure. The

identical AquaB submersible NB generator was used, albeit powered by mains electricity via an AC-DC conversion, with a transformer overhead of ~ 2 W, and a 48 V DC, ~ 0.05 mA current draw.

The temperature, in both laboratory and pilot cases, was ~ 20 $^{\circ}$ C. Measurements were carried out in triplicate.

3. Water Characterisation in the Absence and Presence of EF-ONBs and UV

The pH, oxidation reduction potential (ORP), and dissolved oxygen (DO) of the water samples were measured during and after NB generation, with a portable WTW multi-parameter instrument (WTW multi 3630 IDS, Norderstedt, Germany). In the case of the DI water (in the smaller volume of 5 litres, as a cylinder of 10 cm in diameter and about 16 cm deep of water), the size distribution and concentration of the produced EF-ONBs were measured via a Zetasizer Pro (Malvern) via dynamic light scattering, with the 633 nm laser source light; it was not possible to perform this DLS analysis in the case of shellfish farm water (whether on a 5- or 3500-litre basis), as there was a large degree of background, light-scattering debris in the nano- to micro-scale size range, meaning that having a relatively scatter-free background sample was just not reasonable or possible. A Mettler Toledo probe was used to measure traditionally dissolved ozone (via gas-permeable membrane). In any event, all of the DI water DLS measurements were carried out at a constant temperature (room temperature $\sim 25 \pm 1$ $^{\circ}$ C) through a temperature controller, installed on the system.

In the case of the 5-litre samples using solar-powered EF-ONB generation, the level of dissolved O₃ (and oxygen) was measured over time by titration methods in order to assess any potential extension of dissolved O₃ and O₂ by way of magnitude and time resilience—in view of EF-ONBs potentially overcoming these previously mentioned fundamental barriers.

4. Norovirus-Assessment Methodology

In the case of shellfish farm water, live oysters at a packing density of three per litre were placed in “nano-ozoneated/UV-treated” shellfish farm water, and compared to an identical volume of farm water and number of oysters by way of the ISO-15216 test [27]; RNA was extracted from the oysters’ digestive glands, and quantified by reverse-transcription quantitative PCR (RT-qPCR).

5. Reactive Oxygen Species Generation Study

The formation of reactive oxygen species (ROS)—and, more specifically, hydroxyl radicals (\cdot OH)—was investigated using a specific molecular probe of terephthalic acid (TPA). When exposed to \cdot OH radicals, TPA undergoes hydroxylation, leading to a strong photoluminescence emission at approximately 425 nm. This emission served as an indicator of the presence of hydroxyl-type ROS [28]. To study this investigation, TPA was administered into ‘control’ shellfish farm water not exposed to EF-ONBs and that where such NBs had been created (with and without parallel UV exposure). After 24 h, 3 mL of both the control and sample group solutions (homogenised by shaking) was pipetted for PL measurements, and their respective intensity was recorded using a Cary Eclipse Fluorescence spectrometer.

6. Results and Discussion

Water Characterisation

The size distributions of the electric field-based O₃ nanobubbles (EF-ONBs) in DI water had concentrations of $1.02 \times$ and 0.94×10^9 mL⁻¹, in the absence and presence of UV exposure, respectively, as depicted in Figure 2; respectively, they demonstrated sharp peaks at around 92 and 102 nm. It is possible to influence, to some extent, the size of the nanobubbles by judicious application of various voltages, as this affects the levels of electrostriction on the rising plume of macro- and meso-bubbles by controlling the electric field intensity experienced at the bubble–water interfaces. The goal of the present work is focused on exploring O₃-NB effects, in light of the background application

of UV; as such, a study of the variation in bubble size, and control thereof via applied voltage (or field intensity) manipulation, is not a key goal of the present work. Nonetheless, the present respective findings of ~92 and 102 nm are typically smaller than most NB sizes found in typical mechanical generation approaches [23], which shows already the utility of the electrostriction approach; certainly, the better surface area-to-volume ratio afforded by such smaller sizes leads to improved mass transfer efficiency performance [24], which is also useful for nano-ozonated water to control bioprocesses by penetration into intracellular matrices.

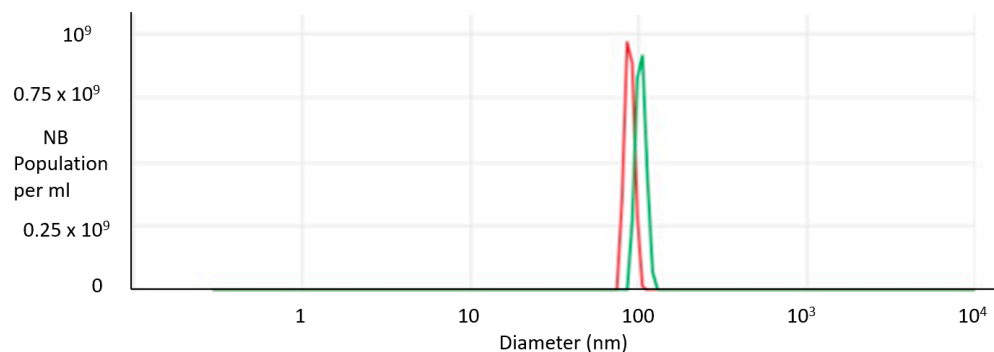


Figure 2. DLS size distributions for EF-ONBs in DI water just after the cessation of NB generation and UV exposure (if applied); red is without UV, whilst green is with.

In any event, this slightly larger size (102 vs. 92 nm) and ~6% population drop in the case of parallel UV exposure suggests that UV treatment acts to catalyse the release of O_3 from the nanobubble state to (individually) solvated molecular form (i.e., a Henry's law state). Although the pH of both the untreated DI and NB-DI water samples (with/without parallel UV exposure) stayed in the range of neutral (between 7 and 7.5), the pH was slightly lower in the 24 h following the EF-ONB creation (about 0.1 units), owing to a higher level of air and dissolved oxygen being maintained in the water—including CO_2 from air and associated carbonic acid. This has also been observed for EF-NBs on a longer-term basis of weeks to months [22,29], although, given the O_3 -centric focus of the present study, the observation period was not extended beyond about 24 h after EF-ONB generation (with or without UV exposure). In the case of the shellfish farm water, the downward pH shift in the case of EF-ONB generation was also of the order of about 0.1 units, being persistent over the observation period below that of no NB generation.

On the other hand, the dissolved oxygen (DO) level in the EF-ONB water consistently exhibited higher levels after the test period compared to the control state of no NB/UV treatment—whether for DI or farm water. Introduction of EF-ONBs into the liquid led to a significant increase in both O_3 and O_2 uptake, surpassing Henry's law saturation levels for DO (i.e., O_2) in contact with atmospheric air at 20 °C, as illustrated in Table 1. In the case of UV application, the level of DO rose to about 130% of Henry's law within ~2 h and stabilised thereafter, whilst a ~125% level was reached after ~4.5–5 h in the case of no parallel UV exposure. This outcome in Table 1 aligns with expectations, as application of UV appears to accelerate the release of O_3 from the NB state and into the individually solvated (i.e., Henry's law state), as well as the general O_3 -to- O_2 auto-dissociation process (also acting to boost DO levels, before their eventual—and very slow—metastability-driven reductions back below Henry's law supersaturation by combined Ficks' and Stokes' law action—albeit to occur, no doubt, over days and longer, as previous EF-air-NB has shown—cf. refs. [22,29]); once again, it is to be borne in mind that the timescale of relevance for the present O_3 -centric study is no more than about 24 h. The Henry's law level for DO here is defined as that in equilibrium with air at the prevailing temperature [22], as the tanks were in all cases open to atmosphere. There are temporary increases above the Henry's law supersaturation levels in DO (which must be understood as isolated O_2 molecules surrounded by their respective hydration layers), which a standard DO probe can measure

(as opposed to not being able to measure O_2 or O_3 in the nano-phase). These temporary boosts in probe-measured DO (which do not take into account, in particular, additional oxygen in “nano-dissolved” form) arise due to the combined effect of O_3 converting into O_2 and additional O_2 in the O_3 gas feed stream (which, of course, is not pure O_3 , and contains elevated O_2 levels compared to air). This has the effect of temporary supersaturation in DO above Henry’s law, which is more dramatic than many other ozonation systems, which may achieve much more modest DO supersaturation for much shorter, transient periods.

Table 1. DO in DI and farm-water (FW) samples just after NB generation, and over time afterwards (% Henry’s law), specifying the standard errors.

	t = 0	2 h	6 h	24 h
DI (control)	73.2 ± 0.8	74.1 ± 0.8	74.4 ± 0.9	74.8 ± 1.0
DI (NB only)	101.1 ± 1.5	113.1 ± 1.7	126.4 ± 1.9	118.8 ± 2.0
DI (NB and UV)	103.2 ± 1.4	129.1 ± 1.6	131.4 ± 1.8	120.6 ± 1.9
FW (control)	77.1 ± 0.9	78.2 ± 0.8	79.0 ± 1.1	79.7 ± 1.0
FW (NB only)	103.0 ± 1.4	114.2 ± 1.6	128.0 ± 1.8	122.1 ± 1.7
FW (NB and UV)	104.5 ± 1.3	131.2 ± 1.7	132.9 ± 1.7	122.4 ± 2.0

There has been very little study in the ozonation literature of O_3 NBs, and even less so in the context of studies of parallel UV application, especially with a view to minimising parallel UV exposure. Refs. [23–26], although studying ozonation via bubbling (typically micro-bubbles and larger nanobubbles—arguably in the small microbubble range instead [23])—do not address to any meaningful extent the parallel presence of UV, and certainly not the more subtle (and vital) point about boosting process energy and operational efficiency by reducing the level of applied UV exposure. For instance, ref. [25] advocates fine-bubble usage to reduce the ozone dosage, whilst ref. [26] strives for overall process energy efficiency by self-powered O_3 generation—which, although relevant to the present study at a high level, do not offer insights into reducing UV irradiation processes by using novel ozone and effective ozone nanobubbling strategies.

Turning to the oxidation reduction potential (ORP), this is a useful “field-metric” [29] for oxidative and ROS activity, and is often used in the field, outside of the scientific laboratory, as a very useful—if imperfect—proxy measure to roughly gauge changes in, *inter alia*, dissolved O_3 (in both the conventional sense, as well as “nano-dissolved” in NB form), and, indeed, overall quality, by way of oxidative potential (in the absence of direct titration analysis, as was undertaken for the 5-litre samples—*vide infra*). This is recorded in Table 2, and it is clear that the EF-ONBs alone achieve substantial boosts in ORP with much less impact from parallel UV exposure. This is highly interesting in an operational strategy sense, as it signals the need for substantially less (energy-intensive) use of UV in parallel with EF-ONBs to achieve a desired level of ORP in improving farm-water quality. This elevated level of ORP, arising mostly from EF-ONBs—as opposed to from parallel UV exposure—echoes (albeit more dramatically) ORP increases seen for EF-air NBs [29]; this is hardly surprising, given that dissolved O_3 from EF-ONBs is a far more potent oxidising agent than from their air equivalents (i.e., EF-ANBs [22,29]).

Considering direct titration to measure the (total level of) dissolved O_3 , although this is challenging owing to some level of ambiguity of whether titration can fully measure the extent of “nano-dissolved” O_3 beyond that of the traditionally dissolved state [21]—with this ‘universal’ caveat/remark applied to any dissolved guest/gas species, and not just O_2 or O_3 —the reader is referred to Figure 3 for the time-dependent results over 6 h after EF-ONB generation (and UV exposure, if applied) is switched off. The level of nano-dissolved O_3 (or, for that matter, oxygen) is calculated by simply subtracting the probe-determined level from the titration-determined quantity, and this gives a reasonable gauge (albeit perhaps a slight underestimate) of the mass concentration in the nano-phase. It is clear that

the approximately exponential decay is slowed down by almost ten times by EF-ONBs without UV applied, and that it is still roughly six times longer than the ‘control’ case of standard O_3 sparging in water (i.e., meso- and macro-bubbles with no meaningful level of dispersed-phase, bubble-mediated dissolution beyond the standard Henry’s law state—owing mostly to rapid Stokes’ law rising speeds). The application of UV, unsurprisingly, hastens the decay of the EF-ONBs, as seen by the lower population and smaller bubble size (cf. Figure 2). In any event, UV applied or not, the presence of O_3 in NB form, and the slower auto-decay to O_2 in that “gaseous” milieu with fewer collisions, albeit with other O_3 molecules in gas-density proximity, compared to individually solvated O_3 molecules with 20 water molecules in the immediate hydration shell coordination layer of the individually solvated state, comes as little surprise.

Table 2. ORP (mV) of DI and FW samples just after NB generation and 2 h later, specifying standard errors.

	$t = 0$	2 h
DI (control)	352 ± 3.2	349.1 ± 2.9
DI (NB only)	423.1 ± 3.9	418.3 ± 3.8
DI (NB and UV)	428.2 ± 4.0	425.0 ± 3.8
FW (control)	283.2 ± 3.0	280.9 ± 2.8
FW (NB only)	378.4 ± 3.5	371.3 ± 3.2
FW (NB and UV)	384.2 ± 4.1	374.6 ± 3.7

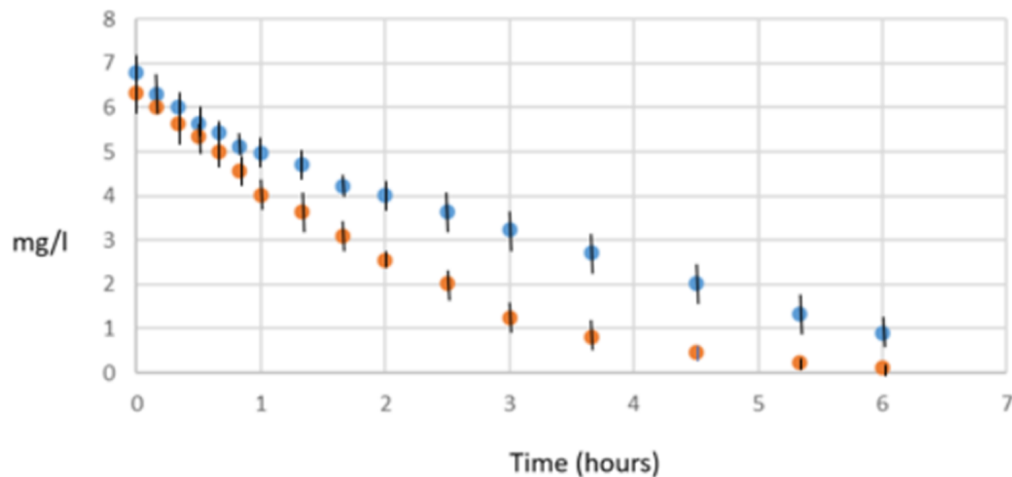


Figure 3. Dissolved O_3 level, by titration, in DI water: blue is NBs only, orange is NBs and UV. Standard errors are shown for points.

7. Norovirus Assessment

The farm-water samples were then stocked with live oysters (just after EF-ONB formation, with and without parallel UV exposure), as well as a control-water case (with the same oyster stocking, but with neither NB formation nor UV exposure), to have their norovirus assessment levels, from RNA extraction after 24 h in the various farm-water samples—as detailed in Table 3. It is clear that there is a very considerable level of reduction from “nano-ozonation” alone (i.e., the additional level of O_3 in the form of nanobubbles, determined approximately in terms of mass concentration by subtracting the probe-measured dissolved O_3 concentration from that determined via titration approaches), and that the additional benefit from UV exposure is minor. Although, of course, this ISO-15216 testing approach, like most PCR-type analysis, is rightly criticised for not discriminating between live and dead (or viable and unviable) viral loads [30,31], the boost in ORP from EF-ONBs,

tailored with probable (although, admittedly, conjectured) entry of these NBs into the oyster gland cells themselves via their cell-wall membranes, leads to effective and long-lived (cf. Figure 2) O_3 penetration to come into direct contact with the intra-cellular virus. Bearing in mind such a substantial effect, it appears that nano-ozonation, without much UV, is effective—although this is preliminary and incomplete, owing to no distinction between live and dead viruses.

Table 3. Norovirus concentration (gc/g), with standard errors.

FW (control)	183 \pm 17
FW (NB only)	84 \pm 5
FW (NB and UV)	78 \pm 6

8. ROS from Photoluminescence

Investigating the impact of EF-ONBs on ROS (so as to be more direct and rigorous than using less reliable proxies like ORP, despite ORP's clear field testing and operational/industrial utility), terephthalic acid (TPA) was introduced as a specific molecular probe for detecting hydroxyl radicals ($\cdot OH$) [32]. TPA was added to all water samples (DI and farm water, with and without EF-ONB/UV application). Although there are some detection errors possible with TPA addition, it has been shown to be a relatively robust approach towards ROS level determination [32]. It was found that the EF-ONB water samples without UV exhibited the most pronounced photoluminescence emission indicative of elevated ROS levels, although parallel UV exposure led to slight levels of diminution therein—but still substantially increased vis-à-vis the “control-sample” state, whether for DI or farm water (cf. Figure 4). The extra availability of (total) dissolved O_3 , even when auto-dissociating (more slowly) to O_2 inside EF-ONBs, does lead to a greater probability of leaked electrons from the electron transport chain [33] creating ROS by reaction collisions with more O_3 and O_2 [29,34], although the O_3 will be inherently more reactive in ROS stimulation.

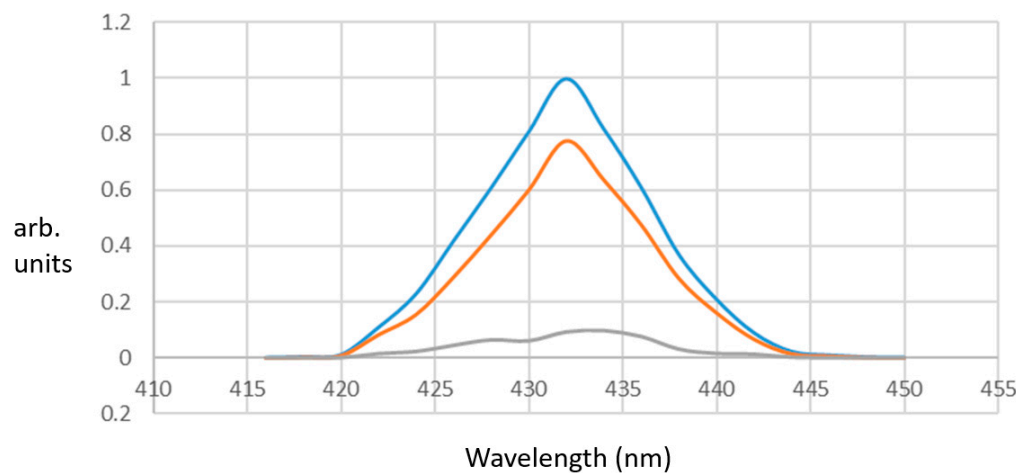


Figure 4. Photoluminescence intensity of terephthalic acid (TPA) exposed to water samples after 24 h in DI water. Blue is EF-ONB without UV, orange is with, and grey is the background control (with neither).

9. Conclusions

This study demonstrates the potential of EF-ONBs (themselves generated in a novel and facile way, with solar power as a viable and attractive option) to greatly enhance the oxidative capacity of water for its disinfection and treatment—using substantially less parallel (and, of course, energy-/maintenance-intensive) UV exposure. This original approach of combining state-of-the-art EF-ONBs (and low-energy, solar-powered/off-

grid approaches to generate them, involving dipolar alignment [35]) with lessening of the level of parallel UV exposure (to the point of elimination thereof) is striking in its wide-ranging implications. These original findings are very important in boosting the operational and energy efficiency of O₃/UV processing in disparate fields, such as, *inter alia*, aquaculture, malting, and advanced oxidation processes in a whole suite of water-treatment operations, ranging from industrial to agricultural and ammonia-prone slurries (e.g., in chicken and pig farming). However, apart from UV irradiation, the attraction of EF-ONBs *per se* in overcoming more fundamental barriers of boosting dissolved O₂/O₃ levels and greater dissolved O₃ longevity (perhaps using ORP as a pragmatic and rough “field-metric” thereof) is very important to highlight. If anything, this is the real “driver” into making ozonation a more sensible, economic, and operationally feasible option for a wider array of (waste-) water applications, beyond the degradation of organic chemicals in industrial wastewater—either with or without parallel UV exposure (and, where UV is required, with substantially reduced levels thereof). Certainly, penetration of longer-lived O₃-NBs through cell-wall matrices in fish and plants and other living organisms and microbes is of interest to help inactivate harmful intra-cellular viruses that are undermining and hampering the health and productivity of (gas-, e.g., oxygen-, consuming) biological systems. This would certainly be the case for RAS systems in aquaculture and shellfish-virus control, as well as for O₃ cycles as part of recycled-water flow management within optimally healthy and productive indoor agriculture systems, and, more recently, for the health and wellbeing of biological communities in barley malting, where cycled-ozonation strategies can make important productivity and homogenising contributions in the intricate orchestration and synchronisation of a complex chain of events.

More broadly, one must bear in mind the residence time of the process at play (e.g., exposure of shellfish to ozonated waters and the lifetime of ozone NBs inside fish and their intra-cellular matrices), so as to ensure that these are (somewhat) less than the “fine-bubble-engineered” dissolved-gas saturation timescales—thereby realising canny and efficient “just-enough” ozonation strategies, so as to also minimise gas supply and bubble-generation operating costs. In this way, one can focus more on the exciting finding of the present study of being able to manipulate and control applied UV inventory to achieve “just-enough” ozonation and associated oxidative reactivity and optimise operating energy costs for ozonation processes in various different settings.

Funding: This research was funded by the European Innovation and Research Councils (under Horizon Europe 190166658 and 101095098, respectively).

Data Availability Statement: The data is included in the article.

Acknowledgments: The author thanks AquaB Nanobubble Innovations Ltd. for the supply of a solar-powered, O₃-compliant submersible nanobubble generator.

Conflicts of Interest: The author declares no conflict of interest.

References

1. Qu, X.; Brame, J.; Li, Q.; Alvarez, P.J.J. Nanotechnology for a Safe and Sustainable Water Supply: Enabling Integrated Water Treatment and Reuse. *Acc. Chem. Res.* **2013**, *46*, 834–843. [[CrossRef](#)] [[PubMed](#)]
2. Rodriguez, C.; Van Buynder, P.; Lugg, R.; Blair, P.; Devine, B.; Cook, A.; Weinstein, P. Indirect potable reuse: A sustainable water supply alternative. *Int. J. Environ. Res. Public. Health* **2009**, *6*, 1174–1209. [[CrossRef](#)] [[PubMed](#)]
3. Policy Dossier on ‘Long-Term 1 Enhanced Surface-Water Treatment Rule’. Available online: <https://nepis.epa.gov/Exe/ZyPDF.cgi?Dockey=30005ZHV.txt> (accessed on 16 June 2024).
4. Zieliński, W.; Korzeniewska, E.; Harnisz, M.; Hubeny, J.; Buta, M.; Rolbiecki, D. The prevalence of drug-resistant and virulent *Staphylococcus* spp. in a municipal wastewater treatment plant and their spread in the environment. *Environ. Int.* **2020**, *143*, 105914. [[CrossRef](#)] [[PubMed](#)]
5. Monteiro, S.; Santos, R. Incidence of enterococci resistant to clinically relevant antibiotics in environmental waters and in reclaimed waters used for irrigation. *J. Water Health* **2020**, *18*, 911–924. [[CrossRef](#)]
6. Rosenberg, S.A.; Goldstein, R.E.; Micallef, S.A.; Gibbs, S.G.; Davis, J.A.; He, X.; George, A.; Kleinfelter, L.M.; Schreiber, N.A.; Mukherjee, S.; et al. Methicillin-Resistant *Staphylococcus aureus* (MRSA) Detected at Four U.S. Wastewater Treatment Plants. *Environ. Health Perspect.* **2012**, *120*, 1551–1558.

7. McKinney, C.W.; Pruden, A. Ultraviolet disinfection of antibiotic resistant bacteria and their antibiotic resistance genes in water and wastewater. *Environ. Sci. Technol.* **2012**, *46*, 13393–13400. [\[CrossRef\]](#)

8. Ding, W.; Jin, W.; Cao, S.; Zhou, X.; Wang, C.; Jiang, Q.; Huang, H.; Tu, R.; Han, S.F.; Wang, Q. O₃ disinfection of chlorine-resistant bacteria in drinking water. *Water Res.* **2019**, *160*, 339–349. [\[CrossRef\]](#)

9. Aguilar-Alarcón, P.; Zhrebker, A.; Rubekina, A.; Shirshin, E.; Simonsen, M.A.; Kolarevic, J.; Lazado, C.C.; Nikolaev, E.N.; Asimakopoulos, A.G.; Mikkelsen, Ø. Impact of O₃ treatment on dissolved organic matter in land-based recirculating aquaculture systems studied by Fourier-transform ion cyclotron resonance mass spectrometry. *Sci. Total Environ.* **2022**, *843*, 157009. [\[CrossRef\]](#)

10. Zuluaga-Calderón, B.; González, H.H.L.; Alzamora, S.M.; Coronel, M.B. Multi-step O₃ treatments of malting barley: Effect on the incidence of *Fusarium graminearum* and grain germination parameters. *Innov. Food Sci. Emerg. Technol.* **2023**, *83*, 103219. [\[CrossRef\]](#)

11. Sgroi, M.; Anumol, T.; Vagliasindi, F.G.A.; Snyder, S.A.; Roccaro, P. Comparison of the new Cl₂/O₃/UV process with different O₃[−] and UV-based AOPs for wastewater treatment at pilot scale: Removal of pharmaceuticals and changes in fluorescing organic matter. *Sci. Total Environ.* **2021**, *765*, 142720. [\[CrossRef\]](#)

12. John, A.; Brookes, A.; Carra, I.; Jefferson, B.; Jarvis, P. Microbubbles and their application to ozonation in water treatment: A critical review exploring their benefit and future application. *Crit. Rev. Environ. Sci. Technol.* **2020**, *52*, 1561–1603. [\[CrossRef\]](#)

13. Paillard, H.; Brunet, R.; Dore, M. Optimal conditions for applying an O₃-hydrogen peroxide oxidizing system. *Water Res.* **1988**, *22*, 91–103. [\[CrossRef\]](#)

14. Tezcanlı-Güyler, G.; Ince, N.H. Individual and combined effects of ultrasound, O₃ and UV irradiation: A case study with textile dyes. *Ultrasonics* **2004**, *42*, 603–609. [\[CrossRef\]](#) [\[PubMed\]](#)

15. Fei, X.; Li, W.; Zhu, S.; Liu, L.; Yang, Y. Simultaneous treatment of dye wastewater and surfactant wastewater by foam separation: Experimental and mesoscopic simulation study. *Separ. Sci. Technol.* **2017**, *53*, 1604–1610. [\[CrossRef\]](#)

16. Arslan, A.; Topkaya, E.; Bingöl, D.; Veli, S. Removal of anionic surfactant sodium dodecyl sulfate from aqueous solutions by O₃/UV/H₂O₂ advanced oxidation process: Process optimization with response surface methodology approach. *Sust. Environ. Res.* **2018**, *28*, 65–71. [\[CrossRef\]](#)

17. Ku, Y.; Su, W.; Shen, Y. Decomposition of phenols in aqueous solution by a UV/O₃ process. *O3 Sci. Eng.* **1996**, *18*, 443–460.

18. Ikemizu, K.; Orita, M.; Sagiike, M.; Morooka, S.; Kato, Y. Ozonation of organic refractory compounds in water in combination with UV radiation. *J. Chem. Eng. Jpn.* **1987**, *20*, 369–374. [\[CrossRef\]](#)

19. Epelle, E.I.; Macfarlane, A.; Cusack, M.; Burns, A.; Okolie, J.A.; Mackay, W.; Rateb, M.; Yaseen, M. O₃ application in different industries: A review of recent developments. *Chem. Eng. J.* **2023**, *454*, 140188. [\[CrossRef\]](#)

20. English, N.J. Environmental Exploration of Ultra-Dense Nanobubbles: Rethinking Sustainability. *Environments* **2022**, *9*, 33. [\[CrossRef\]](#)

21. English, N.J. Sustainable Exploitation and Commercialization of Ultradense Nanobubbles: Reinventing Liquidity. *ACS Sust. Chem. Eng.* **2022**, *10*, 3383–3386. [\[CrossRef\]](#)

22. Saremi, O.; Tuite, D.; English, N.J. Long-Time water aeration by electrostriction-generated nanobubbles. *AIP Conf. Proc.* **2024**, *3084*, 050002.

23. Seridou, P.; Kalogerakis, N. Disinfection applications of O₃ micro- and nanobubbles. *Environ. Sci. Nano* **2021**, *8*, 3493–3510. [\[CrossRef\]](#)

24. Xia, Z.; Hu, L. Treatment of organics contaminated wastewater by O₃ micro-nano-bubbles. *Water* **2018**, *11*, 55. [\[CrossRef\]](#)

25. Hashimoto, K.; Kubota, N.; Okuda, T.; Nakai, S.; Nishijima, W.; Motoshige, H. Reduction of O₃ dosage by using O₃ in ultrafine bubbles to reduce sludge volume. *Chemosphere* **2021**, *274*, 129922. [\[CrossRef\]](#)

26. Lei, R.; Shi, Y.; Wang, X.; Tao, X.; Zhai, H.; Chen, X. Water purification system based on self-powered O₃ production. *Nano Energy* **2021**, *88*, 106230. [\[CrossRef\]](#)

27. ISO 15216-1:2017; Microbiology of the Food Chain—Horizontal Method for Determination of Hepatitis A Virus and Norovirus Using Real-Time RT-PCR—Part 1: Method for Quantification. ISO: Geneva, Switzerland, 2017.

28. Jannesari, M.; Akhavan, O.; Hosseini, H.R.M.; Bakhshi, B. Oxygen-rich graphene/ZnO₂-Ag nanoframeworks with pH-switchable catalase/peroxidase activity as O₂ nanobubble-self generator for bacterial inactivation. *J. Colloid Interface Sci.* **2023**, *637*, 237–250. [\[CrossRef\]](#)

29. Jannesari, M.; Caslin, A.; English, N.J. Electric field-based air nanobubbles (EF-ANBs) irrigation on efficient crop cultivation with reduced fertilizer dependency. *J. Environ. Manag.* **2024**, *362*, 121228. [\[CrossRef\]](#)

30. Hunt, K.; Doré, B.; Keaveney, S.; Rupnik, A.; Butler, F. A quantitative exposure assessment model for norovirus in oysters harvested from a classified production area. *Microb. Risk Anal.* **2023**, *23*, 100247. [\[CrossRef\]](#)

31. McMenemy, P.; Kleczkowski, A.; Taylor, N.G.H. Modelling norovirus dynamics within oysters emphasises potential food safety issues associated with current testing & depuration protocols. *Food Microbiol.* **2023**, *116*, 104363.

32. Page, S.E.; Arnold, W.A.; McNeill, K. Terephthalate as a probe for photochemically generated hydroxyl radical. *J. Environ. Monit.* **2010**, *12*, 1658–1665. [\[CrossRef\]](#)

33. Jannesari, M.; Ejehi, F.; English, N.J.; Mohammadpour, R.; Akhavan, O.; Shams, S. Triggering triboelectric nanogenerator antibacterial activities: Effect of charge polarity and host material correlation. *Chem. Eng. J.* **2024**, *486*, 150036. [\[CrossRef\]](#)

34. Alber, N.A.; Sivanesan, H.; Vanlerberghe, G.C. The occurrence and control of nitric oxide generation by the plant mitochondrial electron transport chain. *Plant Cell Environ.* **2017**, *40*, 1074–1085. [[CrossRef](#)] [[PubMed](#)]
35. Reale, R.; English, N.J. Dipolar response and hydrogen-bond kinetics in liquid water in square-wave time-varying electric fields. *Molec. Phys.* **2014**, *112*, 1870–1878. [[CrossRef](#)]

Disclaimer/Publisher's Note: The statements, opinions and data contained in all publications are solely those of the individual author(s) and contributor(s) and not of MDPI and/or the editor(s). MDPI and/or the editor(s) disclaim responsibility for any injury to people or property resulting from any ideas, methods, instructions or products referred to in the content.